

Synthesis and Characterization of Nanocrystalline $\text{MnCo}_2\text{O}_{4-\delta}$ Spinel For Protective Coating Application in SOFC

A. Das Sharma, J. Mukhopadhyay and R.N. Basu

Fuel Cell & Battery Division
Central Glass & Ceramic Research Institute, CSIR, Kolkata - 700032, India

Nanocrystalline (40-50 nm) powders of $\text{MnCo}_2\text{O}_{4-\delta}$ spinel have been synthesized through combustion technique at a relatively low temperature. The fuel to oxidant ratio has been optimized by carrying out the combustion reaction under various redox conditions (i.e. varying fuel to nitrate ratio) using different fuels viz., citric acid and glycine. A controlled combustion of the complex gel is achieved under a fuel lean condition using a mixed fuel of glycine and citric acid. Phase pure materials are obtained upon calcination of the ash at a temperature as low as 650°C and the powder can be consolidated to more than 95% of theoretical density at a temperature of only 1100°C. The bulk samples show a linear thermal expansion behaviour (CTE: $13.1 \times 10^{-6} \text{ K}^{-1}$) and a high electrical conductivity ($>100 \text{ S/cm}$ at 800°C). Crofer22APU interconnect plates are deposited with the synthesized powder using electrophoretic deposition (EPD) technique for protective coating application.

Introduction

Over the last two decades, progress in materials development and fabrication techniques has led to the lowering of SOFC operating temperatures to a range (e.g., 700-800°C) where metallic alloys can be utilized in place of the costly ceramic interconnect materials used in high-temperature (900-1000°C) SOFC (1). However, such high-temperature metallic interconnects must be simultaneously oxidation resistant and electronically conductive. In this regard, high chromium ferritic steels (e.g. Crofer22APU) are considered to be most promising. However, in oxidizing atmosphere, the formation of chromia scales on such ferritic steel leads to high contact resistances causing performance degradation (2). In addition, volatile Cr species can be released from the Cr_2O_3 scale that causes poisoning of the cathode layer. Moreover, such Cr_2O_3 scale and volatile Cr species may react with Ba-containing glass ceramic sealants to form solid BaCrO_4 thereby causing poor bonding at the relevant interfaces during long term operation of the stack and its performance degradation (3). Application of a dense protective coating of conductive oxides is one of the widely accepted approaches to enhance oxidation resistance, surface stability and inhibit transport of Cr to the gas-phase (3-6). Such coatings must have adequate conductivity, matching coefficient of thermal expansion (CTE), chemical compatibility with adjacent cell components and stability in air. Ceramic perovskites and spinels have been considered as prospective candidates for this purpose (7). Among the perovskites, pure and doped lanthanum chromites (8-9), strontium doped lanthanum manganite (10, 11); lanthanum cobaltite (12) and lanthanum

ferrite (13, 14) have been studied extensively for such coating applications. However, being mixed ionic – electronic conductors, oxide ions can permeate through the coating of many such perovskites to oxidize the metal substrate (14-16). Recently, spinels having the general formula of AB_2O_4 have found widespread attention for such coating application (7, 17). One of the major advantages of the ceramic spinels is that the requisite properties e.g., electrical conductivity and coefficient of thermal expansion (CTE) can be tailored through proper choice of the A and B cations and their stoichiometry to be suitable for coating application. Generally, such spinel powders have been synthesized through the conventional solid state reactions between the precursor salts (oxides and/or carbonates) at high temperature (7).

In the present investigation, nanocrystalline powders of $MnCo_2O_{4.8}$ spinel have been synthesized through combustion technique at a relatively low temperature. The fuel to oxidant ratio has been optimized by carrying out the combustion reaction under various redox conditions (i.e. varying fuel : nitrate ratio) using different fuels viz., citric acid and glycine. Powder and bulk samples have been thoroughly characterized for studying the structural, physical and densification behaviour, thermal and electrical properties. Finally for coating application, Crofer22APU plates are deposited with the synthesized $MnCo_2O_{4.8}$ powder using electrophoretic deposition (EPD) technique. Such coatings are characterized through ASR measurement and their effectiveness under SOFC operating condition has been studied through detailed microstructural analysis.

Experimental

The starting materials used in the synthesis were manganese (II) acetate tetrahydrate (99.5%, E. Merck, India), cobalt (II) nitrate hexahydrate (99.5%, E. Merck, Germany), glycine [E. Merck (India) Limited, 99%], and citric acid monohydrate [E. Merck (India) Limited, 99.5%]. Different batches, based on 10 g of the oxide powder, were prepared using stoichiometric amounts of the metal salts dissolved together in deionized water. Calculated amounts of glycine and citric acid are added to the mixed solution in such a manner so as to vary the redox conditions through a variation in the fuel to nitrate ratio (stoichiometric, fuel lean and fuel rich). While a single fuel (either glycine or citric acid) was used for maintaining stoichiometric fuel to nitrate ratio, a mixture of glycine and citric acid has been used for the fuel lean and fuel rich batches.

The solution mixture, taken in a glass beaker, was allowed to evaporate slowly on a hot plate at around 200°C with continuous stirring. The liquid slowly turned viscous and began to set into a deep black gel and finally auto ignited (the nature of which depend on the fuel composition), leaving behind a light, and fragile mass, called ash. The ash, thus obtained, was calcined between 600 and 750°C for 4 h in air. The calcined powder was ground in an agate mortar and pestle under acetone medium for about 15 min, to break any soft agglomerate, dried, and then pelletized in the form of rectangular bars of dimensions 25 mm × 10 mm × 2 mm under a uniaxial pressure in the range of 175 to 200 MPa. The pelletized bars were finally sintered in the temperature range between 1150 and 1350°C for 6 h in air.

A number of techniques were used for thorough characterization and analysis of the powders and sintered bars. Thermo gravimetric analysis (TGA) was performed on the

corresponding gel samples using a thermal analyzer (STA 409C, Netzsch, Bavaria, Germany). X-ray crystallographic studies were carried out using an X-ray diffractometer (PW 1710, Phillips, Eindhoven, the Netherlands) with Cu-K α radiation. Rietveld refinement of the diffraction data was carried out by PANalytical X'Pert High Score software using a pseudovoigt function. Surface area analysis was carried out on a BET isotherm surface area analyzer (Quantachrome, Nova, USA). The morphology of the calcined powders was determined using transmission electron microscopy (TEM) (Tecnai G² 30 ST, FEI, USA). For this purpose, the specimens were prepared by dispersing the powders in isopropanol upon ultrasonification for about 10 min, deposition on C films, followed by drying under vacuum. The densities of the sintered samples were determined using the Archimedes technique. The grain morphologies of the fracture surfaces of sintered samples were investigated using a scanning electron microscope (430i, LEO, Cambridge, U.K.). The electrical conductivities of the samples in air were measured from room temperature to 1000°C by a four-probe technique using an 8.5 digit multimeter (3458A, HP, Santa Clara, CA). A dilatometer (DIL 402C, Netzsch, Germany) was used to measure the coefficient of thermal expansion (CTE) of sintered samples from room temperature to 800°C.

For coating application, Crofer22APU plates (Thyssenkrupp, Germany) of dimension 10 mm \times 10 mm \times 1 mm are taken for deposition with the calcined MnCo₂O_{4- δ} powder using electrophoretic deposition (EPD) technique. After deposition, the samples are dried and then placed in the furnace and heat treated under different conditions of dwelling time and temperature followed by area specific resistance (ASR) measurement of the coating.

Results and Discussion

Thermal Decomposition of the Gel and Evolution of Phases

As mentioned in the previous section, several batches of nominal composition MnCo₂O_{4- δ} have been prepared to optimize the fuel to oxidant ratio. Thus, the combustion reaction has been carried out under various redox conditions using different fuels (Table I). As shown in Table I, it has been observed that under stoichiometric redox conditions, the reaction is either too vigorous when glycine is used as fuel (1MnCo) or very sluggish when citric acid is used as the fuel (3MnCo). However, a mixed fuel of glycine and citric acid gives a more controlled reaction. Thus, while a fuel rich condition gives a relatively slow burning (2MnCo), a fuel lean condition produces a more controlled reaction (4MnCo). These observations are commensurate with the TGA plots of the corresponding gels from the respective batches (Fig. 1). Consequently, all subsequent experiments were restricted to the 2MnCo and 4MnCo batches only.

Batch ID	Fuel used	Redox Condition	Nature of reaction
1MnCo	Glycine	Stoichiometric	Too vigorous
2MnCo	Glycine+ Citric acid	Fuel rich	Slow burning
3MnCo	Citric acid	Stoichiometric	Very sluggish
4MnCo	Glycine + Citric acid	Fuel lean	Controlled burning

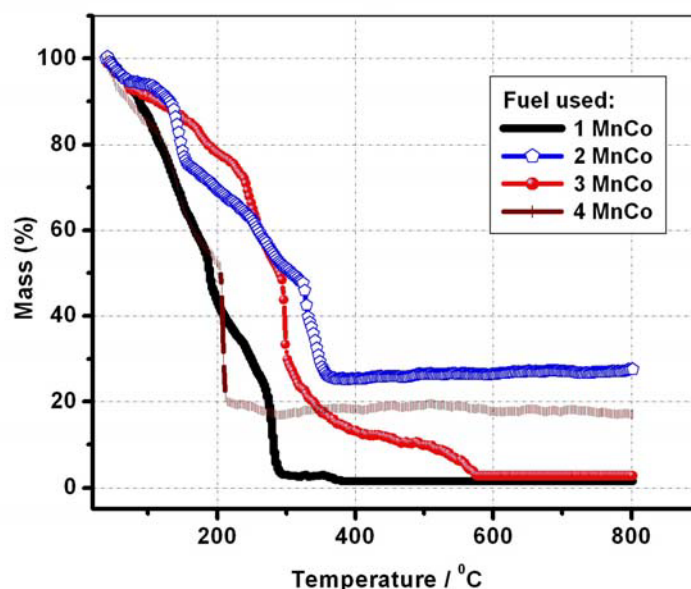


Figure 1. Thermal decomposition behaviour of the gels.

Figure 2 shows the XRD pattern of the as synthesized powder and the calcined (700°C for 4 h) powder. It can be seen that phase evolution begins in the as formed powder itself. Phase pure materials are obtained upon calcination of the ash at a temperature as low as 650°C (figure not shown). The peaks in the 700°C calcined powder could be matched to that of cubic MnCo_2O_4 spinel structure having symmetry group $Fd3m$ (as per JCPDF File No. 023-1237) with a theoretical density of 5.564 g/cc. From the XRD pattern (Fig. 2), the lattice parameter ('a') for the unit cell was found to be 8.1946 Å and 8.2744 Å in case of the precursor ash for the calcined powder respectively. The latter value is in close agreement with that of the theoretical value (8.269 Å as per File No. 023-1237).

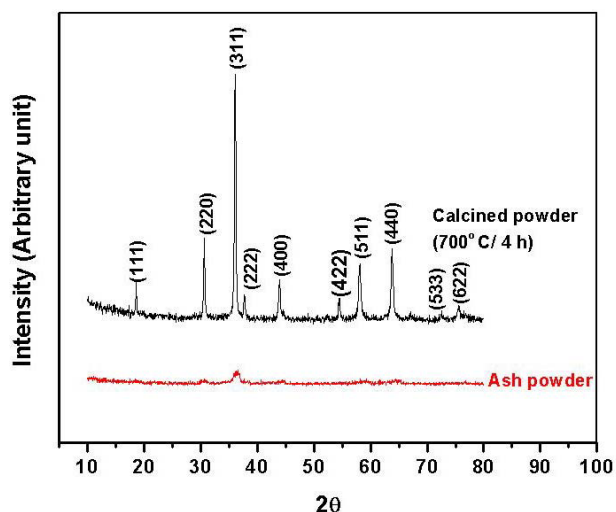


Figure 2. X-ray diffraction patterns of as-synthesized and calcined powders.

Physical Properties and Densification Behaviour of the Powder

BET surface area of the ash and the 700°C calcined powders were measured for the 2MnCo and 4MnCo batches and the results are tabulated in Table II. It is clear from the

Table that the surface area of the ashes are reasonably higher than that of the calcined powders. This is mainly because of soft agglomeration formation during calcination at the high temperature (700°C). Moreover, it was observed that in case of the fuel rich composition (2MnCo) the surface area was higher than that for the fuel lean composition (4MnCo). This may be explained on the basis of the fact that the gel corresponding to 2 MnCo decomposes slowly and requires a relatively higher temperature for complete decomposition (Fig. 1) leading to formation of a less agglomerated structure during subsequent calcination. On the other hand, due to a sharp decomposition at a relatively low temperature for the 4MnCo gel, a more agglomerated structure is formed during calcination of the corresponding ash.

Batch ID	Surface area of ash (m ² /g)	Surface area of calcined powder (m ² /g)
2MnCo	9.926	5.925
4 MnCo	8.552	4.457

Transmission Electron Microscopic (TEM) images of such calcined powders confirms the nanocrystallinity within the synthesized particulates (Fig. 3). It is clear from the figure that the size range of such synthesized powders is found to be within 40 to 50 nm. The agglomerated nature in the calcined powder is also evident from the TEM image.

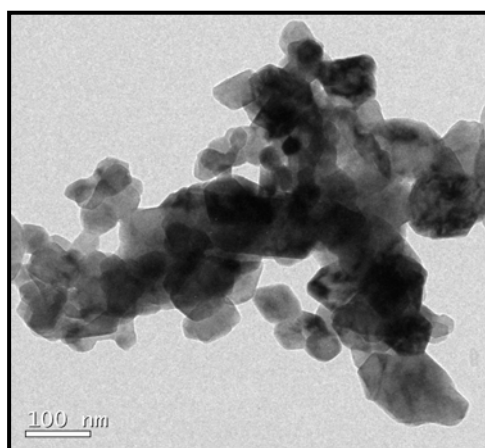


Figure 3. TEM image of 700°C calcined powder.

The densification behavior of the bulk samples prepared under various compaction pressures and sintering temperatures was studied. The compaction pressure was varied between 175 - 200 MPa and the sintering temperature was also varied in the range of 1150 - 1300°C. The variation in density as a function of sintering temperature under two different compaction pressures is shown in Fig. 4. It can be observed from the Fig. 4 that with increase in sintering temperature, the sintered density increases and for a particular sintering temperature, the density is found to be higher at the higher compaction pressure. It is also evident from the figure, that the differential increment of the sintered density obtained at 200 MPa is the lower compared to that for the compaction pressure of 175 MPa. The sintered density is found to be constant (~ 96%) with respect to the increase of sintering temperature in the range of 1150-1300°C. The effect of sintering temperature is found to be more prominent with the bulk compacts made at 175 MPa and the sintered density increases from 93% to 95% upon increasing the sintering temperature in the range of 1150-1300°C.

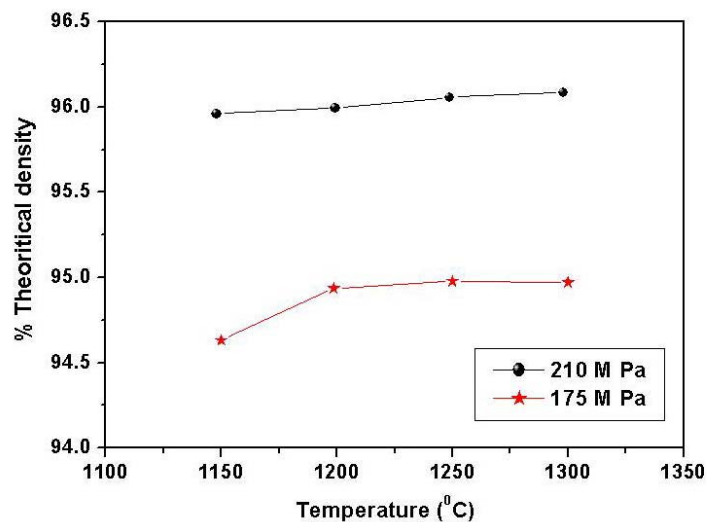


Figure 4. Densification behavior of 2MnCo samples as a function of temperature and compaction pressure.

As, the increment of the sintered density is $\sim 2\%$ (Fig. 4) even at lower compaction pressure of 175 MPa, a reasonably dense sintered microstructure is observed for the spinels sintered at 1150°C. Such a dense fractograph of 4MnCo sintered at 1150°C is shown in Fig. 5. A lower sintering temperature is desirable for the application of the spinel coating at SOFC operational condition which helps the in-situ densification of the applied protective layer.

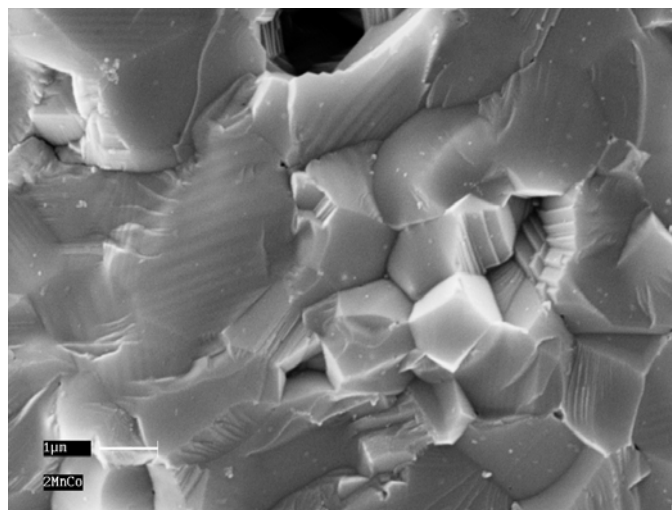


Figure 5. Typical fractograph of a 4 MnCo sintered (1150°C) spinel.

Thermal Expansion Behaviour and Electrical Properties

As shown in Fig. 6, a linear thermal expansion behaviour with an average coefficient of thermal expansion (CTE) of $13.1 \times 10^{-6} \text{ K}^{-1}$ (between 30 and 800°C) is obtained. Thus, the CTE is found to be quite close to that of commonly used metallic interconnects like Crofer22APU (CTE $\sim 12 \times 10^{-6} \text{ K}^{-1}$). It is also evident from Fig. 6 that there is no sudden change in the thermal expansion behaviour indicating that there is no phase transition or transformation of the sample under the range of temperature studied.

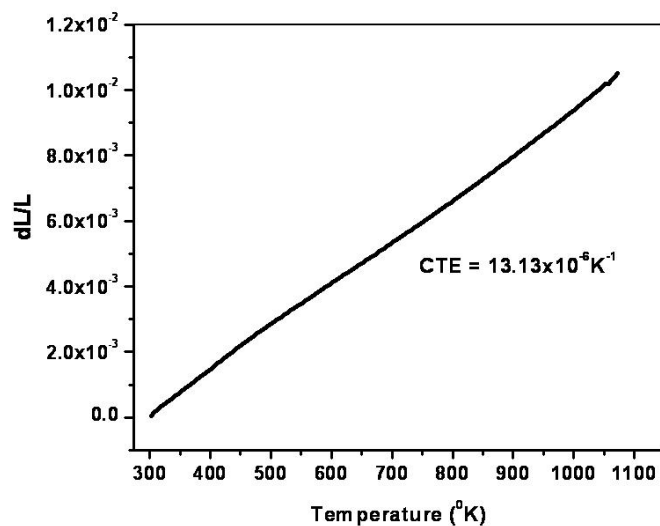


Figure 6. Thermal expansion behaviour of a 4 MnCo sintered (1150°C) spinel.

So far as electrical conduction is concerned spinels are generally believed to conduct by hopping of charge between octahedral sites (17). Thus the presence of different valance states among octahedral cations is beneficial for electrical conduction. Four probe DC electrical resistivity measurement shows a high enough conductivity (>100 S/cm at 800°C) to be suitable for protective coating application. The corresponding Arrhenius plots for the samples prepared under two different redox conditions (viz. 2MnCo and 4MnCo) are presented in Figure 7. A semiconducting type of behaviour with average activation energies of 0.25 eV and 0.33 eV respectively is obtained for the two samples.

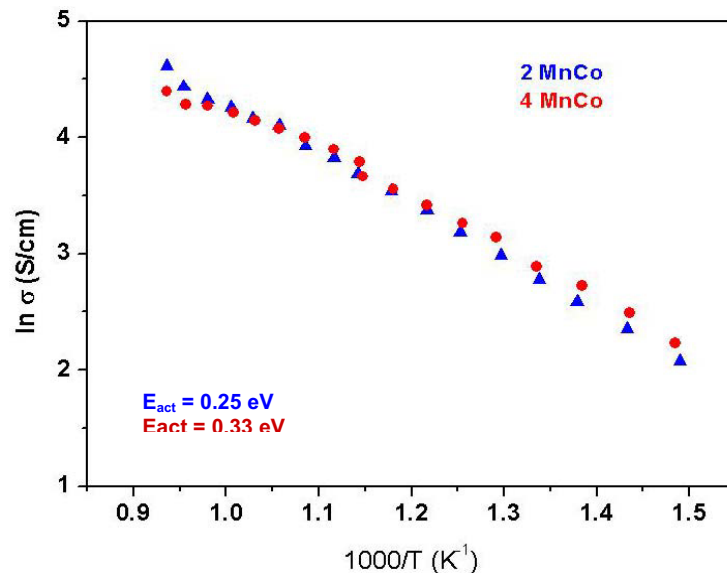


Figure 7. Arrhenius plots of sintered samples of 2MnCo and 4MnCo.

Characterization of the EPD Coating

As already mentioned, for coating application, Crofer22APU plates (Thyssenkrupp, Germany) of dimension 10 mm × 10 mm × 2 mm are taken for deposition with the

calcined $\text{MnCo}_2\text{O}_{4-\delta}$ powder using electrophoretic deposition (EPD) technique. Two types of substrate were used. The first type was heat treated at 800°C in air for 12 h and the second type was sand blasted and no heat treatment was given. After, EPD coating with the 4MnCo powder, both types of the samples were heat treated as per the firing schedule of the SOFC stack operation ($30 - 925^\circ\text{C}$ for 1.5 h and brought down to 800°C and held for 200 h followed by cooling to room temperature). The heat treated coatings were then tested for ASR measurement; a significantly low ASR value of $\sim 1.75 \text{ m}\Omega\text{-cm}^2$ (at 700°C) was obtained for the coating applied on second type of the substrate.

In order to investigate the effectiveness of the coating with respect to minimization of the 'Cr' evaporation, the coated samples were placed over the cathode layer (LSM) of anode-supported single cells of configuration NiO-YSZ/YSZ/LSM-YSZ/LSM under a specific dead load of 1.0 Kg/cm^2 . For comparison, the similar test was performed with uncoated ferritic steel (Crofer22APU). The whole assembly was then heat treated as per the schedule mentioned above. The respective EDAX line scanning of the relevant interfaces of both the samples are shown in Figs. 8 and 9, respectively.

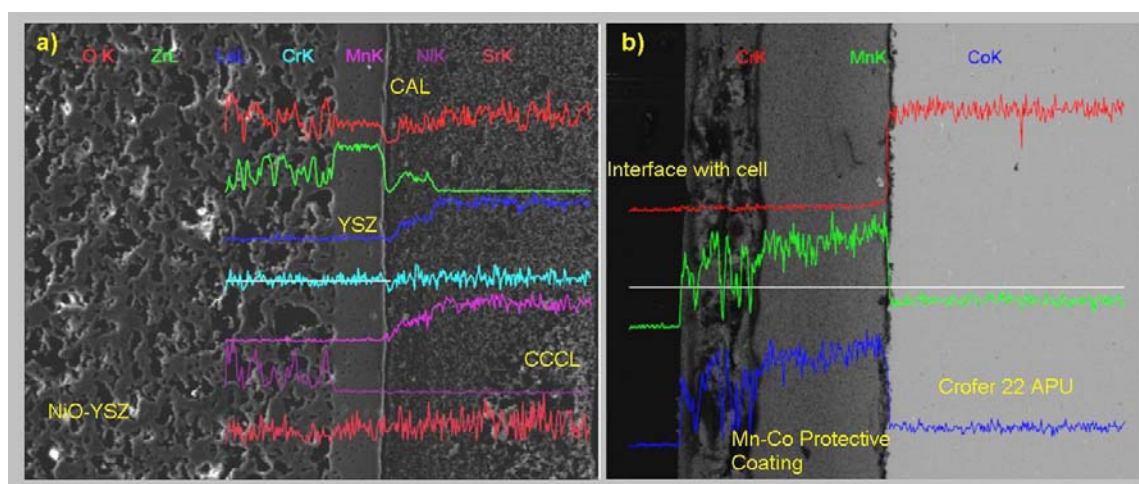


Figure 8. EDAX line scanning of respective elements at different interfaces of single cell (a) and coated Crofer22APU steel (b) [CAL: LSM-YSZ cathode active layer, CCL: LSM cathode current collection layer].

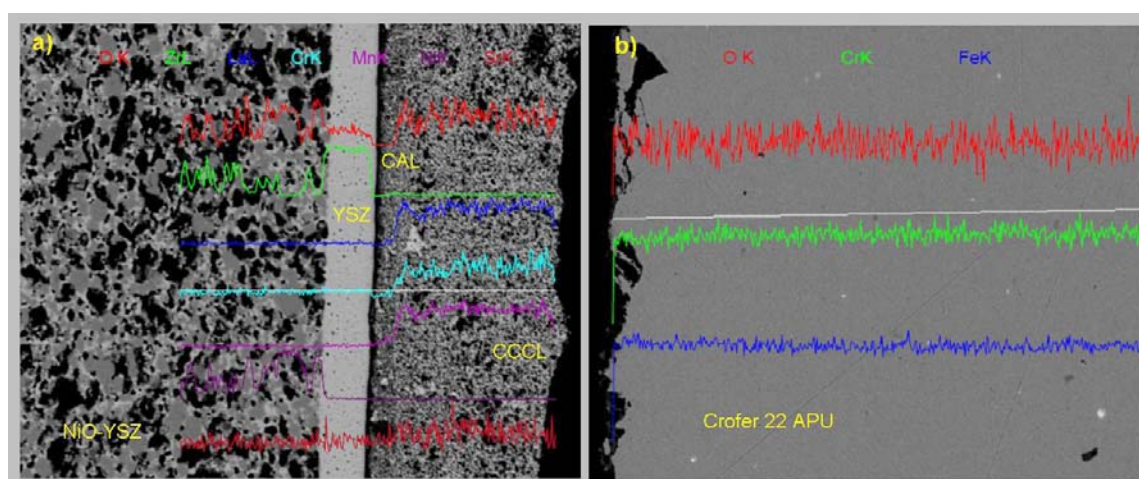


Figure 9. EDAX line scanning of respective elements at different interfaces of single cell (a) and uncoated Crofer22APU steel (b) [CAL: LSM-YSZ cathode active layer, CCL: LSM cathode current collection layer].

It is evident from these figures that substantial amount of 'Cr' loss is restricted upon application of the Mn-Co spinel layer by EPD technique onto ferritic steel of Crofer 22 APU. The line scanning shows the reduction of 'Cr' concentration in the Mn-Co coated layer and thereby reduces the 'Cr' penetration in the cathode layer of the anode-supported single cells

Conclusion

Nanocrystalline powders of $\text{MnCo}_2\text{O}_{4.8}$ spinel were synthesized successfully using soft chemical route like combustion synthesis. Phase pure materials were obtained upon calcination of $\sim 650^\circ\text{C}$. Such materials can be consolidated to $> 95\%$ of theoretical density at a low temperature of $\sim 1150^\circ\text{C}$ and the sintered materials causes high enough electrical conductivity to be used for protective coating application in SOFC. The coating is found to be effective in restricting chromium evaporation from ferritic steel surface to the cathode of single cell.

Acknowledgments

The authors acknowledge Director, CGCRI for his permission to publish the work.

References

1. S. C. Singhal, *Solid State Ionics*, **152-153**, 405 (2002)
2. K. Huang, P. Y. Hou, and J. B. Goodenough, *Solid State Ionics*, **129**, 237 (2000).
3. M. Stanislawski, J. Froitzheim, L. Niewolak, W. J. Quadackers, K. Hilpert, T. Markus and L. Singheiser, *J. Power Sources*, **164**, 578 (2007).
4. Z. G. Yang, G. G. Xia, X. H. Li and J. W. Stevenson, *Int. J. Hydrogen Energy*, **32**, 3648 (2007).
5. W. Qu, J. Li, D.G. Ivey and J. M. Hill, *J. Power Sources*, **157**, 335 (2006).
6. B. Hua, J. Pu, W. Gong, J. F. Zhang, F. S. Lu and J. Li, *J. Power Sources*, **185**, 419 (2008).
7. N. Shaigan, W. Qu, D.G. Ivey, W.X. Chen, *J. Power Sources*, **195**, 1529 (2010)
8. I. Belogolovsky, X. D. Zhou, H. Kurokawa, P.Y. Hou, S. Visco and H. U. Anderson, *J. Electrochem. Soc.*, **154**, B976 (2007).
9. J.H. Zhu, Y. Zhang, A. Basu, Z.G. Lu, M. Paranthaman, D.F. Lee and E.A. Payzant, *Surface & Coatings Technol.*, **177**, 65 (2004).
10. C.L. Chu, J.Y. Wang and S.Y. Lee, *Int. J. Hydrogen Energy*, **33**, 2536 (2008).
11. C.J. Fu, K.N. Sun, N.Q. Zhang and D.R. Zhou, *Rare Metal Mater. and Engg.*, **35**, 1117 (2006).
12. C. Lee and J. Bae, *Thin Solid Films*, **516**, 6432 (2008).
13. Z.G. Yang, G.G. Xia, G.D. Maupin and J.W. Stevenson, *Surface and Coatings Technol.*, **201**, 4476 (2006).
14. X. Montero, N. Jordan, J. Piron-Abellan, F. Tietz, D. Stover, M. Cassir and I. Villarreal, *J. Electrochem. Soc.*, **156**, B188 (2009).
15. C. L. Chu, J. Lee, T. H. Lee and Y. N. Cheng, *Int. J. Hydrogen Energy*, **34**, 422 (2009).
16. N. Shaigan, D. G. Ivey and W. X. Chen, *J. Power Sources*, **183**, 651 (2008).
17. A. Petric and H. Ling, *J. Am. Ceram. Soc.*, **90**, 1515 (2007).